Ilorin Journal of Science
Volume 9, Number 1, 2022, pp. 70 – 85 (Printed in Nigeria)
ISSN: 2408 – 4840 © 2022 Faculty of Physical Sciences, University of Ilorin
https://doi.org/10.54908/iljs.2022.09.01.005

ILORIN
JOURNAL OF SCEINCE

ILJS-22-012

Fluid Substitution-Based Reservoir Studies and Seismic Response in 'Vyshion' Field, Niger Delta

Adeoye[1*], T. O., Sunmonu[2], L. A., Adabanija[3], M. A. and Bayowa[3], O. G.

[1]Geophysics Department, University of Ilorin, Nigeria.
[2]Department of Pure and Applied Physics, Ladoke Akintola University of Technology, Nigeria.
[3]Department of Earth Sciences, Ladoke Akintola University of Technology, Nigeria.

Abstract

A case study of how fluid substitution affects the seismic waveforms is presented. Direct hydrocarbon prediction on the seismic data is prone to inaccuracy without investigating the impact of fluids on the seismic waveforms since the seismic data is influenced by mineral composition, porosity, salinity, pressure, and other factors in addition to fluid type. The study relies on 3D seismic data and log data gathered from 3 wells. Petrophysical and rock physics models were computed in order to understand the seismic dataset. In the analysis, prolific hydrocarbon intervals were identified. Then, model compressional velocities and densities obtained for various fluid scenarios were generated by using the Gassmann fluid substitution theory. Normalized bulk modulus approach was used to reduce the ambiguities that shales portend on the velocity models. Model synthetics were generated. The synthetic seismograms were compared with the seismic dataset in order to understand how fluid saturation and lithology impacts the seismic data. In the analysis, two major hydrocarbon bearing reservoirs were delineated. Other mapped reservoirs have characteristic indices that make them unsuitable for the fluid modelling. The results show that the model oil velocity model better approximates the field velocity. The density models produced the same kind of results, suggesting that the reservoir fluid is oil. The generated synthetic diagrams show that replacing the in-situ fluid with either gas or oil models has no appreciable impact on the seismic dataset's amplitude waveform. This is because seismic reflection amplitude only slightly increases each time gas is assumed. By using the seismic data from this field of study, hydrocarbons cannot be directly predicted from amplitude anomalies because the lithology better influences the seismic waveforms than the fluid composition.

Keywords: Density, Fluid substitution, Reservoir, P-wave velocity, Seismic amplitude, Shaly.

Corresponding Author: Adeoye T.O.
Email: toadeoye@gmail.com

1. Introduction

In Tertiary age sediments, P-wave seismic amplitudes are generally regarded as the most robust direct hydrocarbon indicators. However, in many cases such exploration results in dry holes (Brien, 2010). In essence, there are certain uncertainties associated with directly, identifying hydrocarbon zones on the seismic data. Therefore, the likelihood of obtaining desirable results that will adequately guide economic decisions is diminished unless robust interpretive seismic studies are conducted. Fluid substitution modeling constrained by local field knowledge can improve the understanding of expected polarity of seismic reflectors (Simm and Bacon, 2014). To a great extent, one can also predict fluid content. Fluid substitution is an important part of interpreting seismic data because it helps the interpreter to model the properties of various fluids that can cause an observed seismic amplitude anomaly (Smith *et al.*, 2003). If a reflection amplitude increase or decrease is observed on the seismic section, it might be essential to know whether the event of such peculiarity can be connected to the occurrence of hydrocarbon fluids.

Modeling seismic velocities and densities at a specific reservoir temperature and pressure is the primary goal of fluid substitution by assuming that various fluids are present in the reservoir (Kumar, 2006). The velocities obtained under various fluid assumptions can be compared with the in-situ velocity of primary wave (V_p) or shear waves (V_s). The P-wave velocity is the most important mode of seismic propagation for petroleum exploration because they can travel through solids, liquids and gases (Ashcroft, 2011). Therefore P-wave velocity can be correlated with both fluid and solid materials. Shear (S or secondary) waves travel through solids but not through liquids and gases (Veeken, 2007).

In reservoirs, change in P-wave velocity can be affected by a number of factors. For instance, mineral composition, porosity, salinity, temperature and of course, fluid type. Gassmann equation takes these effects into account, to compute velocity (Avseth *et al*., 2005). This equation links the bulk modulus of a rock to its pore, dry rock frame and fluid properties (Avseth *et al*., 2005). Sometimes, the Biot-Gassmann fluid substitution equation proposed by Biot (1956), can also be used for fluid substitution but, like the Gassmann theory, is limited in some ways (Walls *et al.*, 2004). Biot-Gassmann equations may not be applicable to some given data because at low frequencies, Biot-Gassmann equation reduces to the Gassmann theory and at high frequencies, several authors have discovered that velocity and frequency are not well related because the calculated velocity difference between zero and infinite frequencies is usually less than 3% for most reservoir rocks (Winkler, 1985; Wang and Nur, 1990). Biots's theory can be defined by a set of analytical equations (Biot, 1956; Smith *et al.*, 2003). According to Smith *et al.*, (2003), Gassmann theory is still the most theoretically sound and is widely used in reservoir studies.

Gassmann equation is sequential and different equations are used at different levels. Two important steps are usually taken to apply the Gassmann equation: calculating the bulk modulus of the porous rock frame (K_{frame}- rock drained of any pore-filling fluid) and secondly, computing the bulk modulus of the rock saturated with any desired fluid (K_{sat}) (Smith *et al.*, 2003). The porous rock frame is calculated first because it is an input in the estimation of the

saturated bulk modulus. Bulk modulus is defined as the ratio of hydrostatic stress to volumetric strain that the stress will impact on the rock (Avseth *et al.,* 2005). In other words, it is the resistance of various earth materials to stress. The higher the bulk modulus, the stiffer the rock. However, the bulk modulus (K) for in-situ conditions need to be calculated before one can obtain the bulk modulus of the porous dry frame (K_{frame}). To do this, initial field V_p and V_s velocity must be known (Smith *et al.,* 2003).

It might be essential to check the impact of the fluid substitution velocities and densities on seismic data in order to determine whether it can improve comprehension of the seismic data (Veeken, 2007). This is achieved by using the model velocities and densities as input in the synthetic seismogram generation and this synthetic model is compared at line intersections with the seismic data.

In the field of study, most elastic information available are from laboratory measurements. It is very important to derive log models of these elastic properties as these are more detailed. A comprehensive information of velocity is then available. In addition, the identification of fluids based on the common petrophysical overlay of the neutron and density log is quite ambiguous in a practical sense (Adeoye *et al.,* 2021). Many times, it thus seems that the neutron-density log technique does not deliver reliable results during fluid contact mapping because it is affected by lithology effects (Adeoye *et al.,* 2021). However, the computation of the elastic properties of velocities in the formation and comparison with real field data gives much more straightforward responses.

2. Materials and Methods

The materials used for the study include seismic dataset and well log records from 3 wells but only 2 wells penetrate hydrocarbon zones. Elastic data calculated in the laboratory are supplied in form of velocity data. The study began with quality check of the log data, achieved by removing spikes from the logs and is followed by petrophysical analysis to identify prolific reservoir zones. This involved mapping porous and permeable units using the gamma ray log (GR log), followed by the identification of reservoir fluids using the resistivity log (RES_DEP). Since hydrocarbons are highly resistive, high resistivity anomalies are expected in hydrocarbon sands. For the fluid substitution process, it was essential to use high porosity units. Porosity log is computed from the density log as 'estimated log'. Water saturation log (SW log) is a direct indication of the hydrocarbon fraction and was computed from the Archie's water saturation equation using the resistivity log (Cannon, 2016):

$$S_W = (aR_W / \Phi^m R_t)^{\frac{1}{n}} \quad (1)$$

where

R_w = resistivity of formation water at formation temperature
R_t = true resistivity of formation (i.e. RES_DEP).
Φ = porosity
a = tortuosity factor =1
m = cementation exponent =2, n = saturation exponent = 2

The Gassmann theory, widely used for fluid substitution, can help the reservoir scientists and engineers to understand how the seismic reflection data respond to changes in fluid fill (Smith *et al.*, 2003). Using this equation, fluid substitution modelling was carried out with applications written and embedded in a MATLAB™ derived fluid substitution app. Excel spreadsheet and Petrel™ software were also used in other aspects of reservoir modelling.
Since shale minerals impact velocity models, a cognitive interpretation was necessary. Two steps were followed. The first method is identifying high porosity (0.28-0.35) and thick (>60 ft) hydrocarbon zones with low V_{sh} values. The 2nd is normalizing the velocities of matrix and fluid. The Normalized bulk modulus model is an attempt to control the bulk modulus variables in order to constrain it to follow a minimized V_{sh} trend (Simm. *et al.,* 2003).

Within each prolific reservoir identified, the in-situ fluids were removed and the water saturations values were changed for different modelled fluid scenarios i.e. for oil, gas and brine. The reservoirs were consequently modelled to obtain compressional velocities (V_p) for gas, oil and brine saturations scenarios. These were afterwards compared with field velocity (Field V_p). Then, the saturated density, P was computed for oil, gas and brine model assumptions. These were also compared with the field P.

The product of V_p and P, is the acoustic impedance (AI), which is a very important rock property and needed in mimicking the seismic reflections response (i.e. synthetic seismogram generation).
To generate the compressional velocity, V_p computation over definite intervals, the Gassmann velocity equation below is used:

$$V_P = \sqrt{\frac{K + \frac{4}{3}\mu}{P}} \tag{2}$$

A very significant earth property in that equation is the saturated bulk modulus (K). It is given by the Gassmann theory and expressed below as:

$$K_{sat} = K_{frame} + \frac{\left(1 - \frac{K_{frame}}{K_{matrix}}\right)^2}{\frac{\phi}{K_{fl}} + \frac{(1-\phi)}{K_{matrix}} - \frac{K_{frame}}{K^2_{matrix}}} \tag{3}$$

Density (P) is obtained from the equation 2 as:

$$P_{sat} = \Phi P_{fl} + (1 - \Phi) P_{matrix} \tag{4}$$

where
ϕ = Porosity
P_{fl} = saturating fluid density

P_{matrix} = matrix density

On the other hand, shear modulus μ, is obtained by

$$\mu = PV_S^2 \tag{5}$$

where
P = density defined earlier.
V_s= Shear wave velocity.

In equation 3, K_{frame} is the porous rock frame or dry rock modulus. This is the bulk modulus of the rock drained of any pore-filling fluid. The formula for estimating K_{frame}, proposed by Zhu and McMechan, and highlighted by Kumar (2006) is:

$$K_{frame} = \frac{K_{sat}\left(\frac{\phi K_{matrix}}{K_{fl}} + 1 - \phi\right) - K_{matrix}}{\frac{\phi K_{matrix}}{K_{fl}} + \frac{K_{sat}}{K_{matrix}} - 1 - \phi} \tag{6}$$

where
K_{sat} = insitu saturated bulk modulus obtained from field V_p and V_s data.
K_{fl}= Bulk Modulus of saturating fluid.
K_{matrix} = Bulk modulus of rock matrix.
Φ = Porosity.

Since the pore space in the hydrocarbon unit is typically occupied by two or more fluid systems, inverse bulk modulus averaging method was used for calculating the saturating bulk modulus of fluids that may be present in the system, K_{fl} as:

$$\frac{1}{K_{fl}} = \frac{SW}{K_{brine}} + \frac{HS}{K_{hyc}} \tag{7}$$

where
S_w is the water saturation defined earlier
HS = Hydrocarbon saturation ($1-S_w$).
K_{brine} = is the bulk modulus of the brine and
K_{hyc} = is the bulk modulus of the hydrocarbon phase which depends on the assumed fluid properties of gas, oil or brine.

Additionally, the hydrocarbon reservoir is not made up of only the fluid part and it is therefore essential to calculate the bulk density of rock matrix (K_{matrix}). K_{matrix} was calculated via the

application of Voigt-Ruess-Hill averaging of the mineral constituents of the rock (Avseth *et al.*, 2005):

$$K_{matrix} = \frac{1}{2}\left(\left[V_{clay} K_{clay} + V_{qtz} K_{qtz} \right] + \left[\frac{V_{clay}}{K_{clay}} + \frac{V_{qtz}}{K_{qtz}} \right] \right) \quad (8)$$

where

V_{clay} = Volume of clay = 70% * V_{sh} (V_{sh} is the '*shale volume*' obtained from the Gr Log).

V_{qtz}= Volume of quartz= 1-Vclay

K_{clay} = bulk modulus of clay = 20.9, Gpa obtained from Mavko, *et al* (1998).

K_{qtz}= bulk modulus of quartz =36.6, Gpa also obtained from Mavko, *et al* (1998).

A synthetic seismogram was generated from the well data in order to compare the reflections on it with that of the seismic data. To achieve this, the model densities and velocities were multiplied. Acoustic impedance is thus, calculated as a function of depth and a reflectivity series is generated, derived from approximated Zeoppritz 's equation as discussed by Avseth *et al.*, (2005):

$$\text{Reflectivity Series} = \frac{P_2V_2 - P_1V_1}{P_2V_2 + P_1V_1} \quad (9)$$

In order to generate the model synthetics, the above equation was convolved with a zero phase 'wavelet' domiciled in the Petrel^{TM} software and a synthetic seismogram was created throughout the defined depth interval. The seismic data is labelled "Full". A certain degree of reflection 'correlation' was obtained between the model synthetic and seismic data after a phase rotation of 45º was performed.

3. Results and Discussion

The Gassmann model that was used in this study, assumes that the rock is composed of a single mineral in which the total pore spaces are in communication with one another (Wang and Nur, 1990). This means that, Gassmann equation is not applicable in sands containing significant fractions of shale because the pore spaces cannot communicate with one another. Besides, shaly units are not composed of a single mineral and water that is bounded to the shale minerals cannot move freely. For this study, the reservoir units are mostly sandwiched between shaly sands with moderate to high porosity (Figure 1). These porosity values increases the belief that a reasonable result can be obtained. In Figure 1, the gamma ray (GR), resistivity (RES_DEP), Porosity (Estimated) and water saturation (S_w) logs are displayed in their respective tracks. Using these logs, the productive zone is identified and is highlighted in yellow color. Thus, reservoir zones that are thick, porous, low in shale content and having shale volume between 0.10-0.15, were selected while the non-prolific units are colored in blue (Figure 2). Fluid substitution was not performed in reservoirs that fall short of the above reference criteria. It is thought that thin reservoirs with large shale volumes and low porosity are not of excellent grades (Bacon *et al.*, 2003).

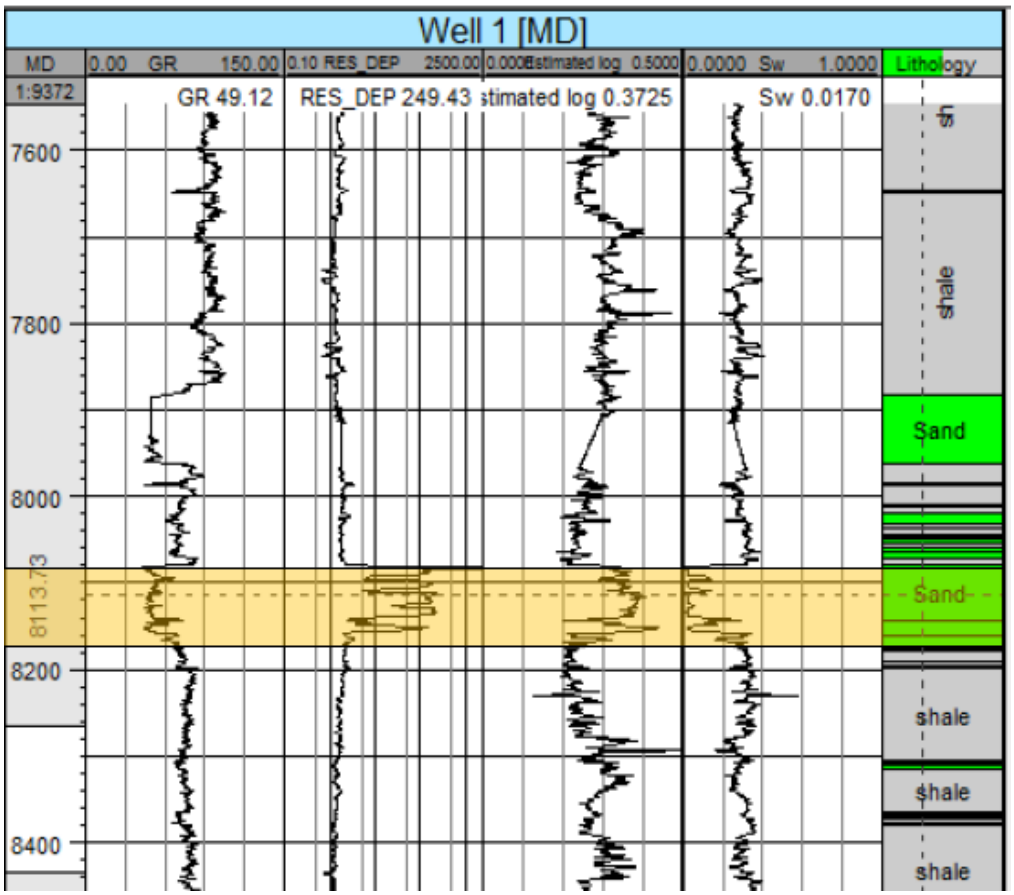

Figure 1: Well Section showing Measured Depth (MD) in feets, Gamma ray log (GR) in API units, Resistivity log (RES_DEP) in Ohm-m, Porosity (Estimated log) in %, Water Saturation (S_w) in % and Lithology Columns.

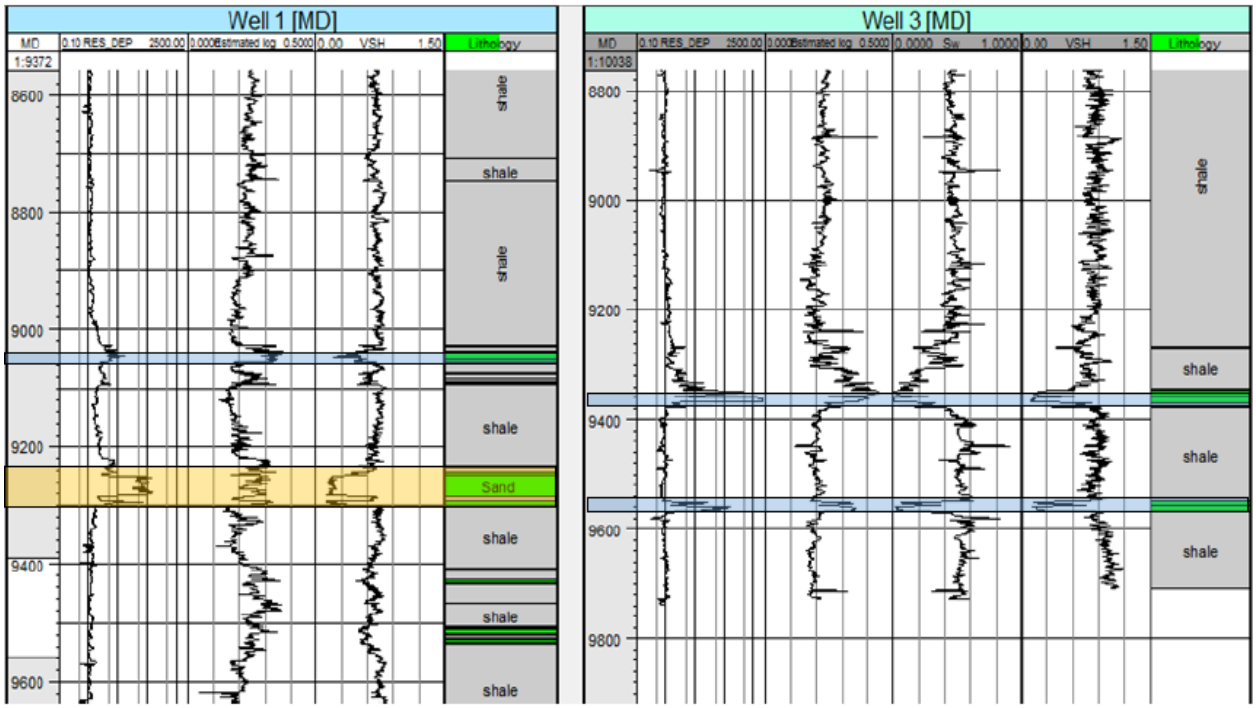

Figure 2: The porosity (Estimated Log), thickness (color shades) and volume of shale (VSH) of Wells 1 and 3 are displayed as the basis for sieving off some reservoir units.

For the productive reservoirs, it was essential to apply the normalized bulk modulus method (Simm and Bacon, 2014). The normalized bulk modulus approach is a crossplot of effective porosity against normalized bulk modulus (Figure 3). K_{fd} is the K_{frame} while K_{m0} is the K_{matrix}. Both were obtained from the Gassmann computation. A mineral trend is obtained on the crossplot by using volume of shale (V_{sh}) values to constrain the model. This (normalized) function is applied to the Gassmann computation and the root mean square (R.M.S) error is calculated (0.0266) (Figure 3).

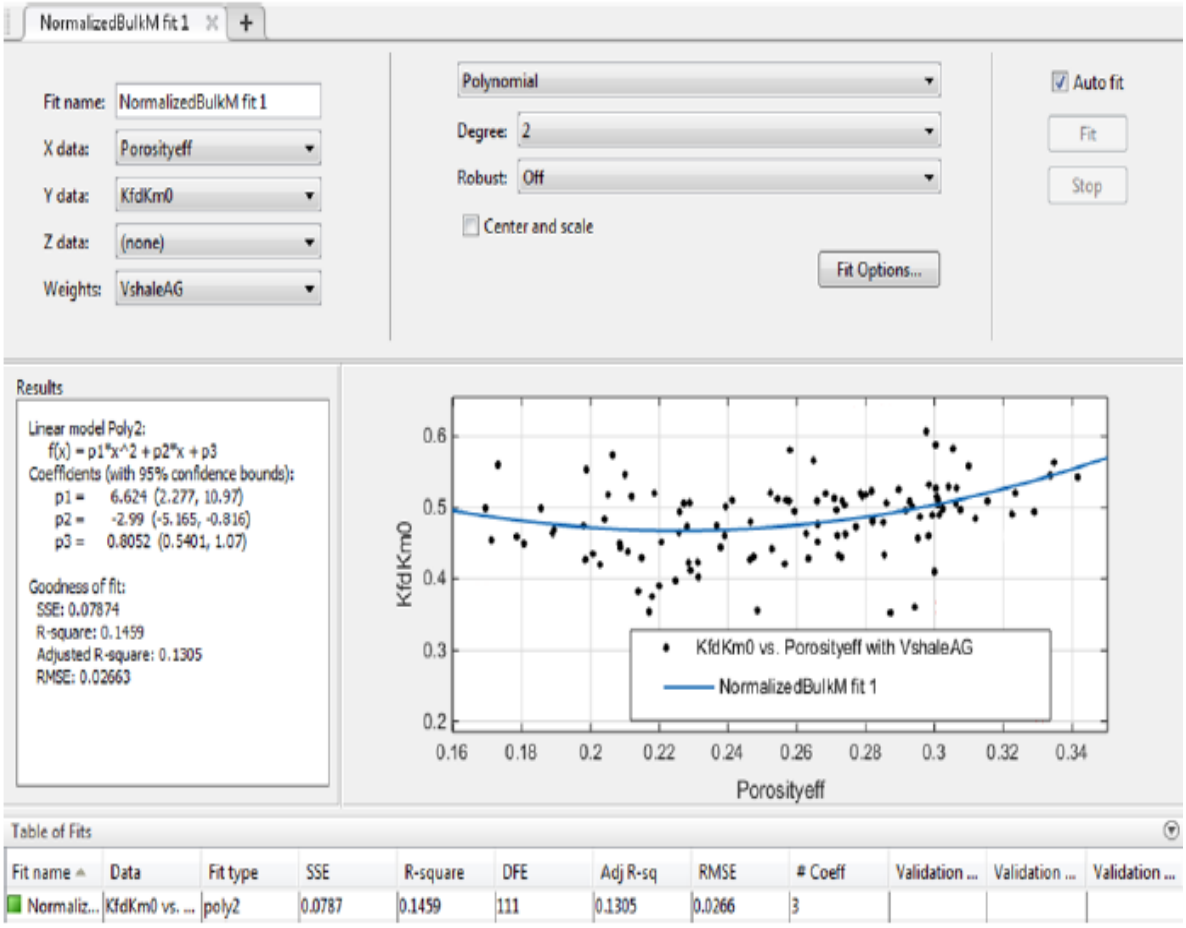

Figure 3: Normalized bulk modulus method showing mineral trend. The R.M.S Error for the fit is low (0.0266).

Figure 4 shows the velocity solutions obtained from the Gassmann equation between depths 8,062 ft and 8,180 ft from well 1. The P- wave velocity for brine, oil and gas fluid scenarios are labelled brine, oil and gas respectively. The profile begins with a drop in velocity. Between 8,109 ft - 8,180 ft, the field V_p tracks the oil velocity curve suggesting that oil is present in the interval. Both oil and gas models are lower than brine velocity (marked in blue color). This is expected.

Figure 5 shows the velocity interval for the 2nd reservoir. Various changes in velocities are observed between depths 9,242 ft and 9,293 ft. In this zone, the V_p for the gas scenario is also lower than that of the oil and brine. Comparisons with field V_p shows that the gas model is essentially close to the field V_p. However, the field V_p tracks the oil velocity more than the gas velocity. This suggests that the reservoir may contain more oil than gas.

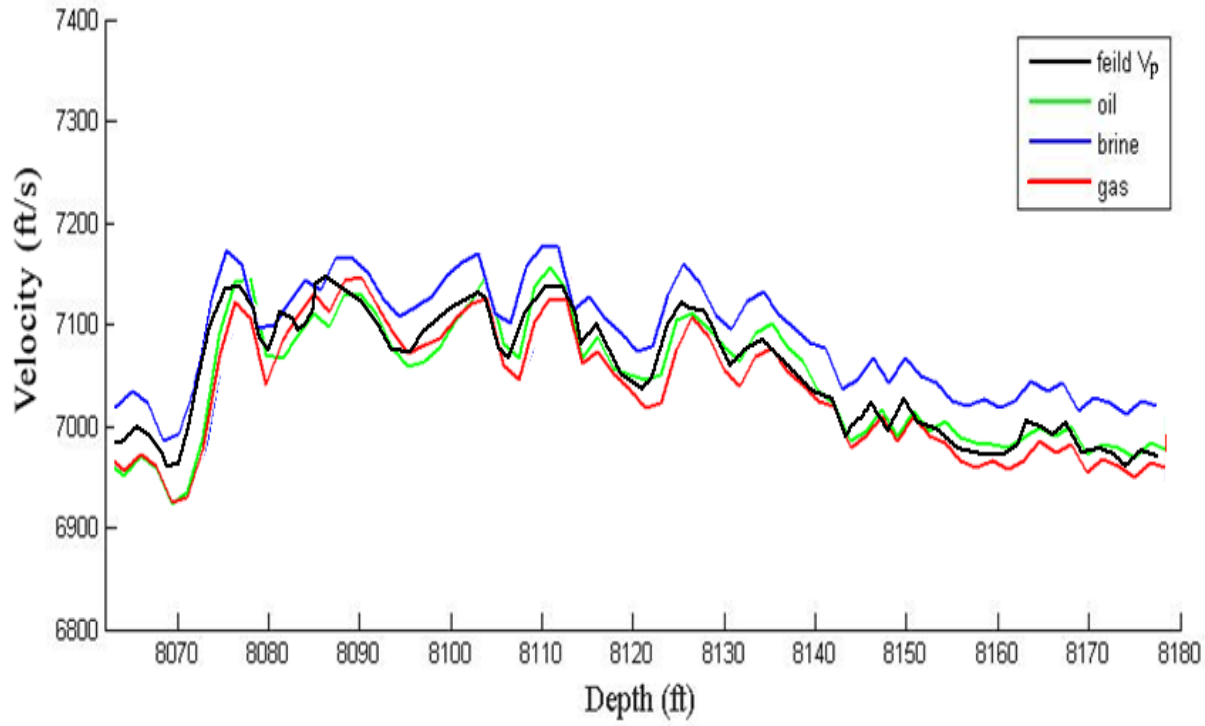

Figure 4: Reservoir interval 1 showing velocity models and field velocity plotted on the same track.

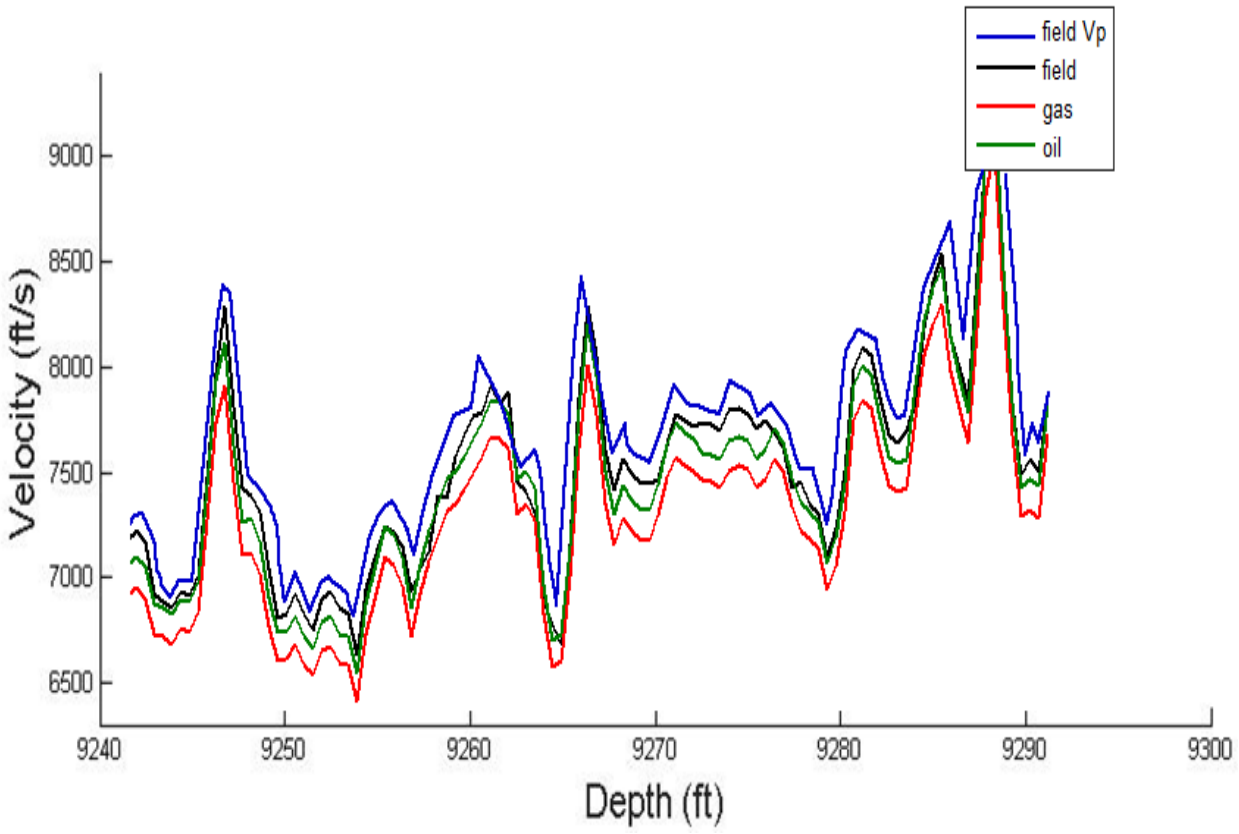

Figure 5: Reservoir interval 2 showing velocity models and field velocity plotted on the same track.

The same procedure is repeated for the density estimation (P) by plotting field density (Field P), gas density (P_{gas}), oil density (P_{oil}) and Brine density (P_{brine}) on the same track (Figure 6). Large differences are observed when the model P_{gas} was compared to the Field P. However the separation is smaller between oil density and Field density. The match between the density of oil and field density suggests that the zone contains more oil than the other fluids.

For the 2nd reservoir, which lies between 9,240 ft and 9,300 ft, the field density is close to P_{oil} between depths 9,250 ft and 9,275 ft (Figure 7). However, they do not track one another. The interval is believed to significantly contain more oil than all other fluids because of the proximity of the oil model to the field data. The Brine density is also close to the in-situ density data between 9,240 ft -9,249 ft and 9,285 ft -9,294 ft. This may suggest that some measure of brine is contained in the zone.

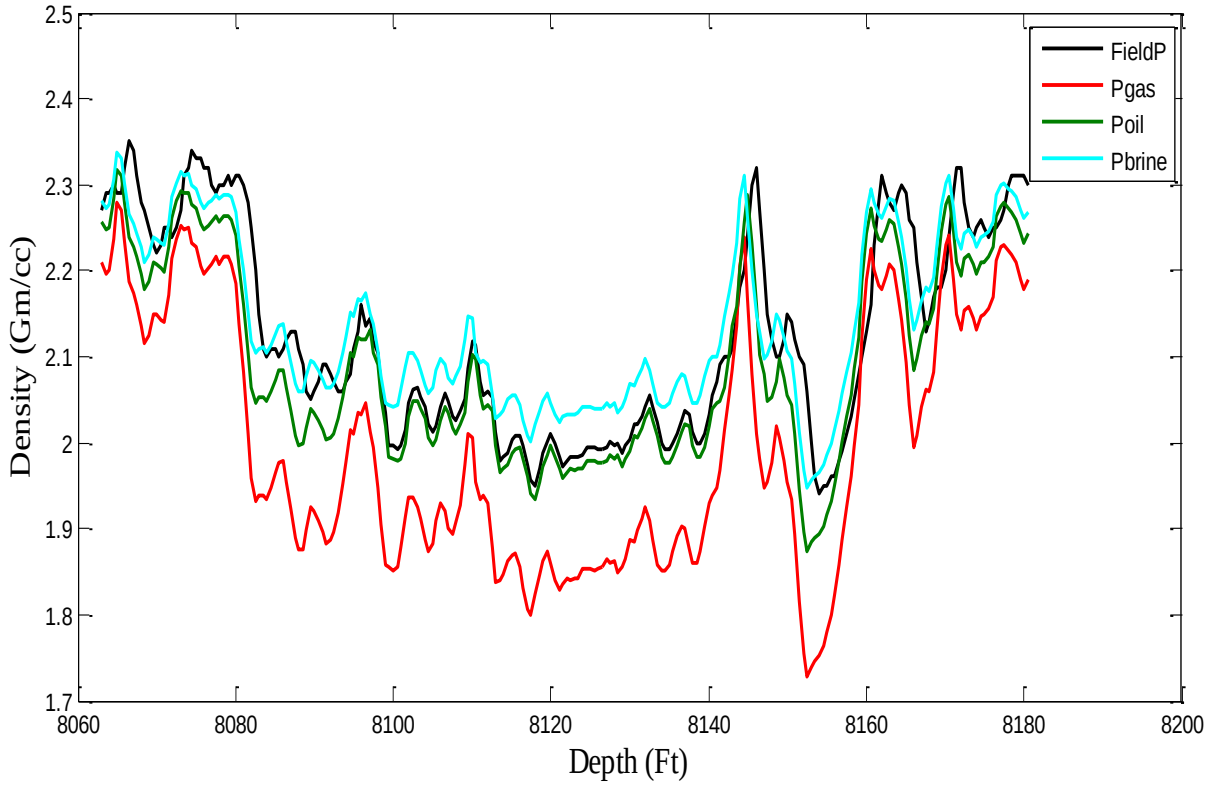

Figure 6: Reservoir interval 1 showing density (P) models and field velocity (Field P) plotted on the same track.

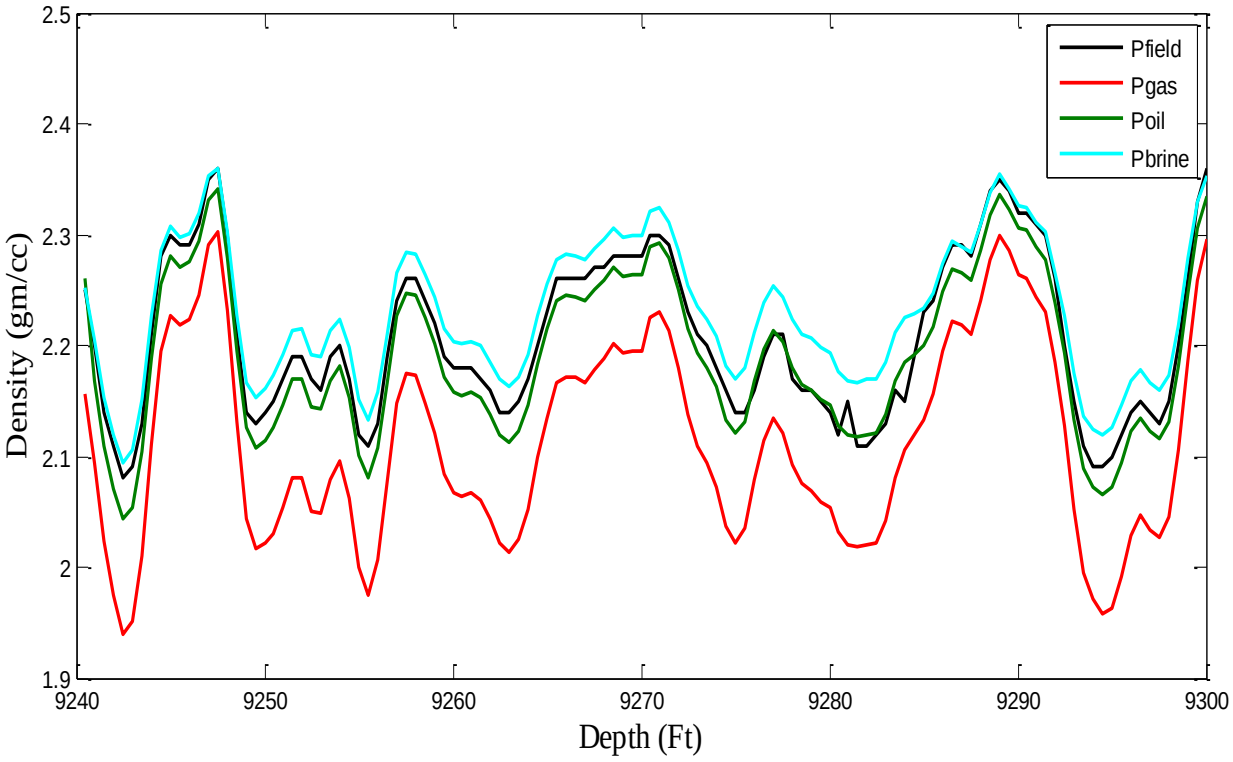

Figure 7: Reservoir interval 2 showing density (P) models and field velocity (Field P) plotted on the same track.

Model synthetics were compared with seismic expressions to understand the impact of model velocities and densities on the seismic data (Figure 8). The blue reflection represents the positive seismic peak. This is the European polarity of seismic data in which the red reflections represent transitions to low acoustic impedance layers. Amplitude changes are observed at the analyzed interval but are not very strong. Care should be taken before they are used as hydrocarbon indicators because the embedding amplitude reflections display identical reflection characteristics e.g. reflections at depths 7,680 ft – 7,720 ft. For the prolific reservoir located between 8,060 ft and 8,180 ft, the observed intercalation of shales within the pore spaces of the reservoir may give rise to multiples that are inherent as scattered reflections on the seismic data. Also, from previous analysis, the assumption is that the hydrocarbon in the interval is presumed to be oil rather than gas. Most fluid indication on the seismic data relates to gas rather than oil reservoirs as the effect on acoustic properties of gas in the pore space is significantly greater than oil (Brown, 2004). In addition, the monotonous nature of the seismic dataset makes the well to seismic match rather ambiguous. However, when model gas saturation is assumed in the reservoir interval and corresponding model velocities and densities of gas are used as inputs, the amplitudes of the reflections increases only slightly (Figure 9). The red/white amplitude reflection is probably as a result of gas sand having a lower impedance than the overlying shale.

On the other synthetic diagrams (Figures 10 and 11), there are no significant amplitude changes as the oil and gas scenarios are assumed respectively. Thus, the effect of various fluid

saturations on the seismic response, majorly depends on the nature of the enclosing layers (shale). Within the reservoir layers, it is believed that significant changes in amplitude would have occurred if the embedding shale units and the reservoir units are sufficiently thicker. This is noted in Figure 11 at depths that are far away from the reservoir interval (8,870 ft- 9,185 ft). The strong blue and red amplitudes of the reflections are as a result of sufficient contrast in impedance between the embedding thick shale and the thin layered shale free reservoir that is located in-between them. As long as there are sufficient contrast in velocity and density values between the embedding medium and the reservoir, high amplitude reflections may be observed (Brown, 2004).

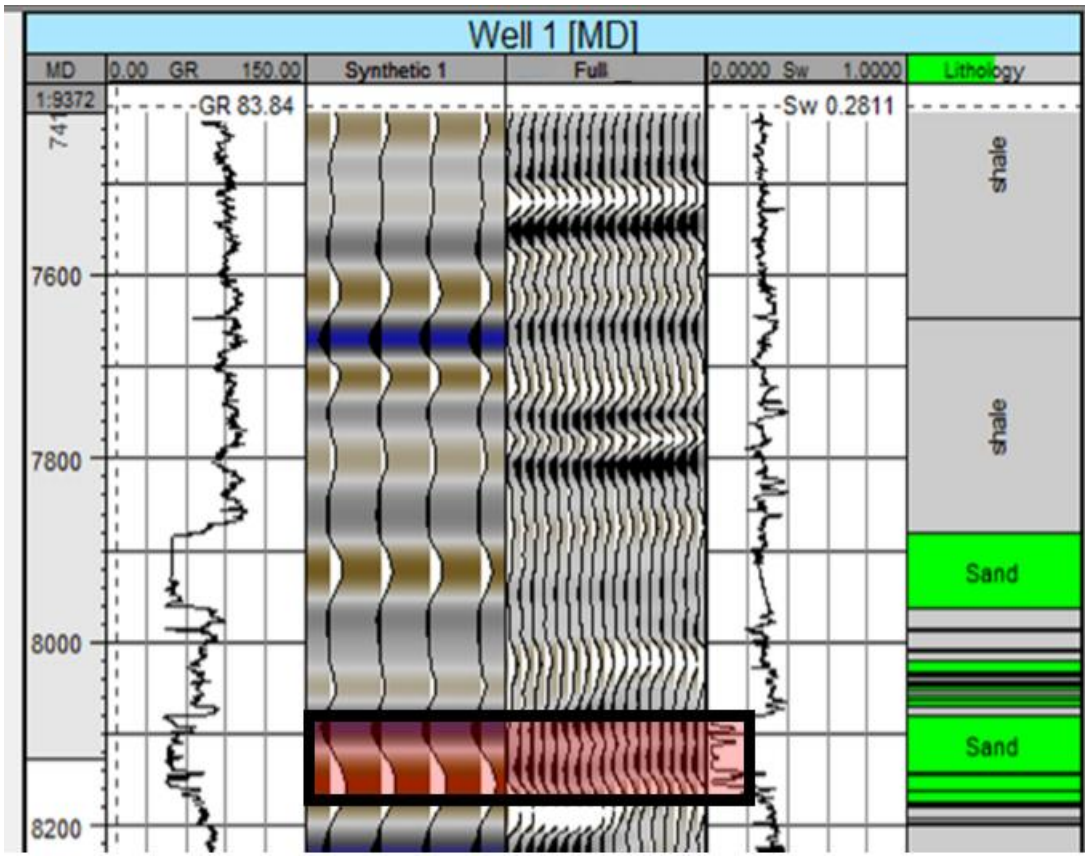

Figure 8: In Reservoir Interval 1, the synthetic seismogram (synthetic 1) for the oil scenario is showed alongside the seismic amplitudes (labelled "Full").

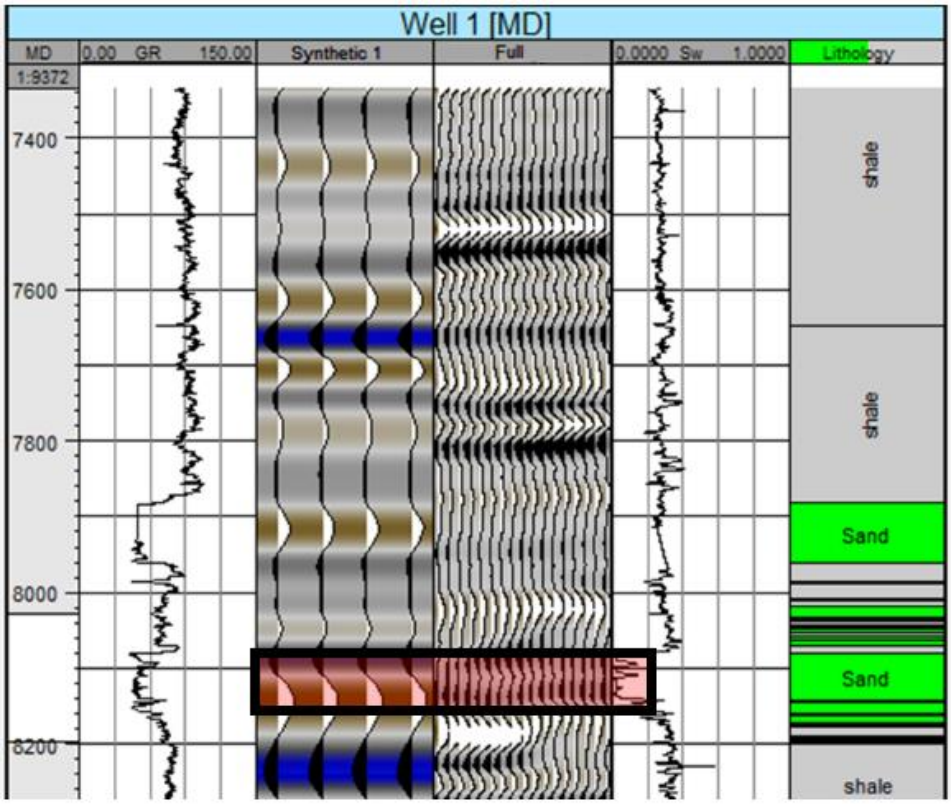

Figure 9: In Reservoir interval 1, the synthetic Seismogram (synthetic 1) for the gas scenario is shown alongside the seismic amplitudes (labelled "Full").

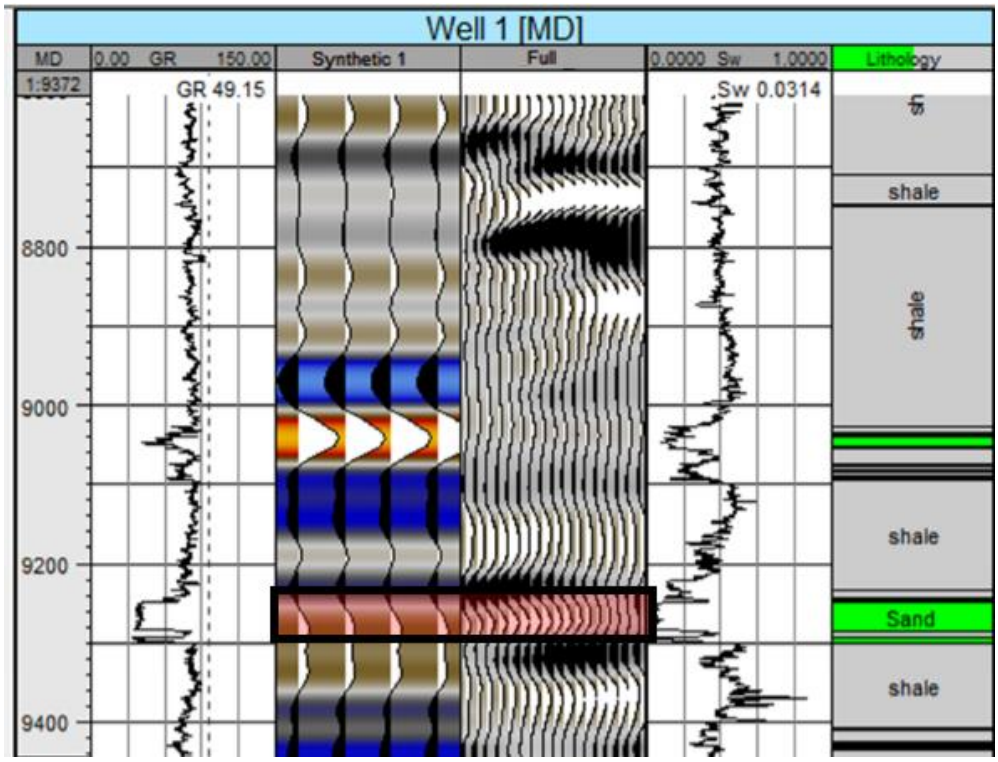

Figure 10: In Reservoir Interval 2, the synthetic Seismogram (synthetic 1) for the oil scenario is showed alongside the seismic amplitudes (Labelled "Full").

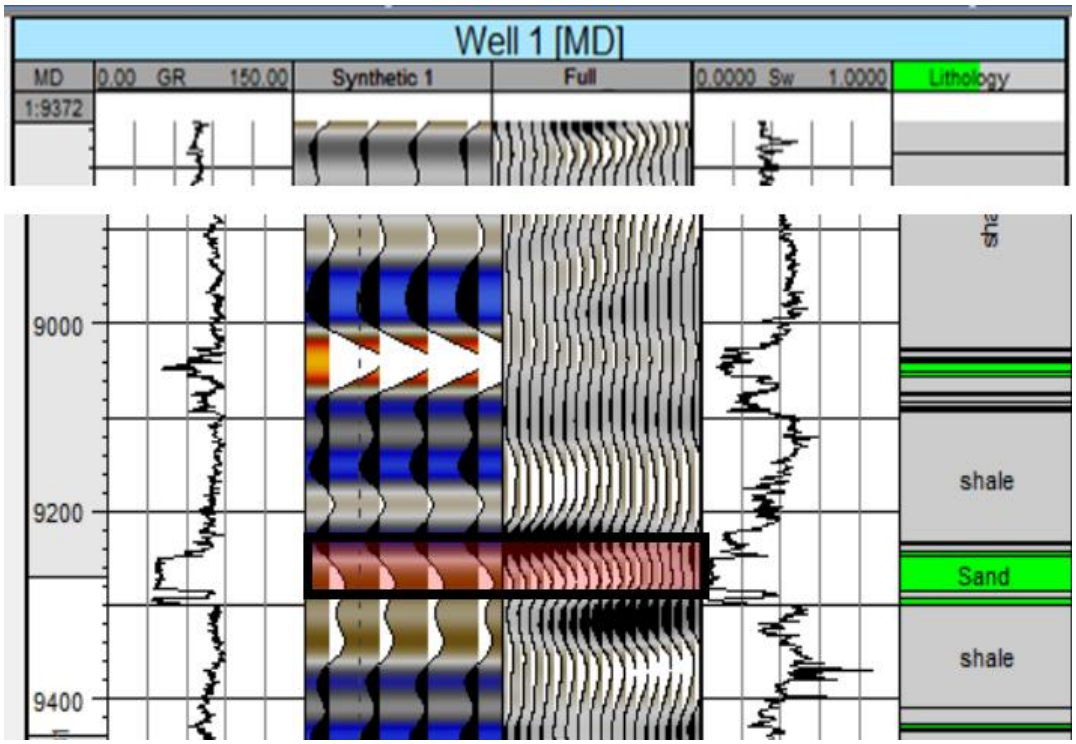

Figure 11: In Reservoir Interval 2, the synthetic Seismogram (synthetic 1) for the gas scenario is showed alongside the seismic amplitudes (Labelled "Full").

4. Conclusion

Hydrocarbon reservoirs were identified in this fluid substitution process. They occur mostly within shaly sands. At some points, the embedding shale are also intercalated with thin sand units. The reservoirs are of high porosity (0.28-0.35). Fluid substitution is performed in the reservoirs with high porosity, high reservoir thicknesses and low volume of shale in order to obtain reliable results using the normalize bulk modulus method. Model velocities and densities were compared with the field velocity.

The model oil velocities obtained from the study matches that of the field data more than the velocities of all other fluids (brine and gas). The model oil densities also show the same trend. The deduction is that more oil is present in the reservoirs than gas or brine.

When the oil-synthetic seismogram was generated using the aforementioned models and compared with the seismic reflection data, the amplitude of the oil-synthetic correlated with that of the seismic data. However, when model gas velocities and densities were substituted for the oil model, the model synthetic is not significantly changed. Outside the reservoir interval, amplitude of reflections increases when thick reservoir sands are embedded within thick shale units. The study therefore, concludes that lithology strongly influences the seismic amplitudes and that the reservoir fluid in the field of study is majorly oil. The seismic response can, thus, be better understood within the context of fluid substitution analysis.

Acknowledgement

The authors acknowledge the technical contributions and revisions of our senior colleagues and friends. The authors also appreciate the efforts of the reviewers of this manuscript and the cordial working relationship with members of staff at the Faculty of Physical Science, University of Ilorin.

References

Adeoye T.O., Raji, W.O. and Ofomola, M.O. (2021): Improved Log Estimation of Porosity and Water Saturation in Shaly Reservoirs - A Niger Delta Case study. *FUW trends in Science and Technology*. 6 (3), 689-693.

Ashcroft, W. (2011): *A petroleum geologist's guide to seismic reflection*, 1st edn., John Wiley & Sons, West Sussex, United Kingdom, 55.

Avseth P., Mukerji T and Mavko G. (2005): *Quantitative seismic interpretation*, 1st edn., Cambridge University Press, New York, 1-89.

Bacon, M., Simm, R. and Redshaw, T., (2003): *3D Seismic Interpretation*, 1st edn., Cambridge University Press, New York, 146-148.

Biot, M.A (1956): Theory of propagation of elastic waves in a fluid saturated porous solid. II. Higher frequency range: *Journal of the Acoustical Society of America*, 28, 179–191.

Brien J.O. (2010): Seismic Amplitudes from low gas saturation sands. In Johnston D.H. (eds.) Methods and Applications in Reservoir Geophysics. SEG investigations in Geophysics. 15, 155-161.

Brown, A. R., (2004): *Interpretation of three-dimensional seismic data*, 6th edn., American Association of Petroleum Geologists, Memoir 42, Oklahoma, U.S.A., 153-160.

Cannon S. (2016): *Petrophysics: A practical guide*, 1st edn., Wiley Blackwell publishing, Chichester, West Sussex, UK, 38-45.

Kumar, D. (2006): A Tutorial on Gassmann Fluid Substitution: Formulation, Algorithm and Matlab code. *Geohorizons Journal of Society of Petroleum Geophycisists*, 4-12.

Mavko, G., Mukerji, T., and Dvorkin, J., (1998): *The rock physics handbook: Tools for seismic analysis in porous media.* Cambridge Univ. Press, New York, 65-75.

Simm, R. and Bacon, M. (2014): *Seismic Amplitude. An interpreter's handbook,* 1st edn., Cambridge University Press, New York, 195.

Smith, T. M., Sondergeld, C. H., and Rai, C. S., (2003): Gassmann Fluid Substitutions: A Tutorial. *Geophysics.* 68, 430-440.

Veeken, P.C.H. (2007): *Seismic stratigraphy, basin analysis and reservoir characterization. Handbook of Geophysical exploration*, 37, 1st edn., *Elsevier*, Oxford, United Kingdom, 388.

Walls J., Dvorkin, J., & Carr, M. (2004): Well Logs and Rock Physics in Seismic Reservoir Characterization. In *Offshore technology conference*. OnePetro. 10-15.

Wang, Z., and Nur, A. (1990): Dispersion Analysis of Acoustic Velocities in Rocks. *The Journal of the Acoustical Society of America, 87* (6), 2384-2395.

Winkler, K. W., (1985): Dispersion Analysis of Velocity and Attenuation in Berea Sandstone: *Journal of Geophysical Research.* 90, 6793–6800.